

**ICSO 2016**

**International Conference on Space Optics**

Biarritz, France

18–21 October 2016

*Edited by Bruno Cugny, Nikos Karafolas and Zoran Sodnik*



***Hypatia: a 4m active space telescope concept and capabilities***

*Nicholas Devaney*

*A. Goncharov*

*M. Goy*

*C. Reinlein*

*et al.*



International Conference on Space Optics — ICSO 2016, edited by Bruno Cugny, Nikos Karafolas,  
Zoran Sodnik, Proc. of SPIE Vol. 10562, 1056235 · © 2016 ESA and CNES  
CCC code: 0277-786X/17/\$18 · doi: 10.1117/12.2296233

Proc. of SPIE Vol. 10562 1056235-1

## HYPATIA -- A 4M ACTIVE SPACE TELESCOPE CONCEPT AND CAPABILITIES

N. Devaney<sup>1</sup>, A. Goncharov<sup>1</sup>, M. Goy<sup>2,3</sup>, C. Reinlein<sup>2</sup>, N. Lange<sup>2,3</sup>

<sup>1</sup>*School of Physics, National University of Ireland, Galway, Ireland*

<sup>2</sup>*Fraunhofer Institute for Applied Optics and Precision Engineering IOF, Albert-Einstein-Str. 7, D-07745, Jena, Germany*

<sup>3</sup>*Institute of Applied Physics, Abbe Center of Photonics, Friedrich Schiller University Jena, Max-Wien-Platz 1, 07743 Jena, Germany*

### I. INTRODUCTION:

While ambitious plans are being developed for giant, segmented telescopes in space, we feel that a large monolithic mirror telescope would have several advantages in the near term. In particular, the risk involved in deploying the optics will be significantly reduced, and the telescope can provide excellent image quality without the need for precise segment alignment and phasing. The diameter of the telescope primary mirror is limited by current rocket fairings to 4 m, and we are developing the concept of such a mission, which we refer to as Hypatia. Hypatia would have a diffraction-limited resolution 1.7 times smaller and a collecting area approximately 2.8 times larger than the Hubble Space Telescope (HST). As a monolithic telescope designed to have excellent image quality down to near UV wavelengths it would be a worthy successor to the HST, allowing for a wide-range of astrophysical missions. Operation at L2 would also increase the sensitivity of the telescope as compared to HST, which operates in low-Earth orbit.

The Hypatia telescope could also have a significant impact on exoplanet studies. The diffraction-limited of Hypatia at a wavelength of 1 micron would be 0.05 arcseconds. An advanced coronagraph (such as a vector coronagraph) could obtain Inner Working Angles practically as small as this, which would surpass the best current ground-based planet hunters, and greatly extend our knowledge of giant (warm) planets. Alternatively, the telescope could operate in conjunction with a starshade – it has recently been shown that the yield of ExoEarths with starshades flattens as a function of telescope diameter for telescopes about 5-6 m. A 4m telescope such as Hypatia would therefore be well suited to this mode of observation [1]. The same study has shown that the yield of ExoEarths with a 4m space telescope and starshade could be of order 10. This is certainly a significant number, given that the first clear identification of an Earth analogue will be one of the most important discoveries ever made! It would also give a first reliable measurement of the frequency of Earth-like planets around different types of stars, including those similar to the sun.

In order to minimize weight we consider that the primary mirror will be lightweight and not have active control, as this would involve the use of several large actuators. Active control is necessary in order to correct for thermal fluctuations, as well as perturbations of the optics due to launch and vibrations due to telescope slews. We propose to carry out the active control using actuation of the secondary mirror, and by re-imaging the primary mirror onto a deformable mirror. In this article we present the optical design concept and initial estimates of the performance of this system. We also outline the deformable mirror concept, while this is described in greater detail in a companion paper in this conference.

### II. OPTICAL DESIGN AND PERFORMANCE:

In our baseline, the telescope employs a Ritchey-Chrétien design. Near the RC focus a fold mirror directs the beam to an off-axis parabola which images the primary mirror onto the deformable mirror (see Fig. 1). The optical pupil of the deformable mirror has a diameter of 110 mm. In order to minimize the number of surfaces, the deformable mirror has a spherical shape with a radius of curvature of 2800 mm, which directly provides the output beam. The complete system provides excellent image quality ( $SR > 0.9$  at  $0.5 \mu\text{m}$ ) over a field of view of  $2.7 \times 2.7$  arcminutes. The final f-number (telescope plus relay optics) is 10.98 – the relay system re-images the RC focus with approximately unit magnification. The Airy disk size at the final focus is 7.4 microns, and the image scale is 0.213 arcseconds per mm.

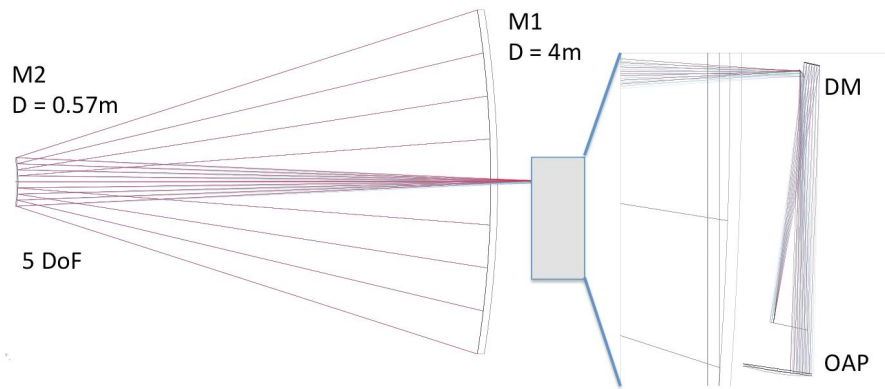


Fig. 1 Optical layout of the HYPATIA Active telescope

We do not have a detailed opto-mechanical simulation of the primary mirror support, and assume a set of Zernike coefficients for the primary mirror aberrations up to Z26 (Tetrafoil9). The coefficients have values of 300 nm rms for both Coma terms, 200 nm rms for the Astigmatism terms, 75 nm rms for spherical aberration, and 50 nm rms for all the higher-order terms. These terms are applied to the primary mirror as a Zernike surface, and the DM shape, which is also modeled as a Zernike surface, is allowed to vary in order to optimize image quality across the field. In addition, the axial position of M2 is allowed to vary to correct for defocus. A wavefront defocus of 3 microns is corrected by moving the secondary mirror by 209 microns. Fig. 2 shows the Strehl ratio at 0.5 microns over the field of view when the aberrations are corrected. The on-axis corrected wavefront error is 22 nm rms, as compared to 10 nm rms before aberrations are added to the primary mirror.

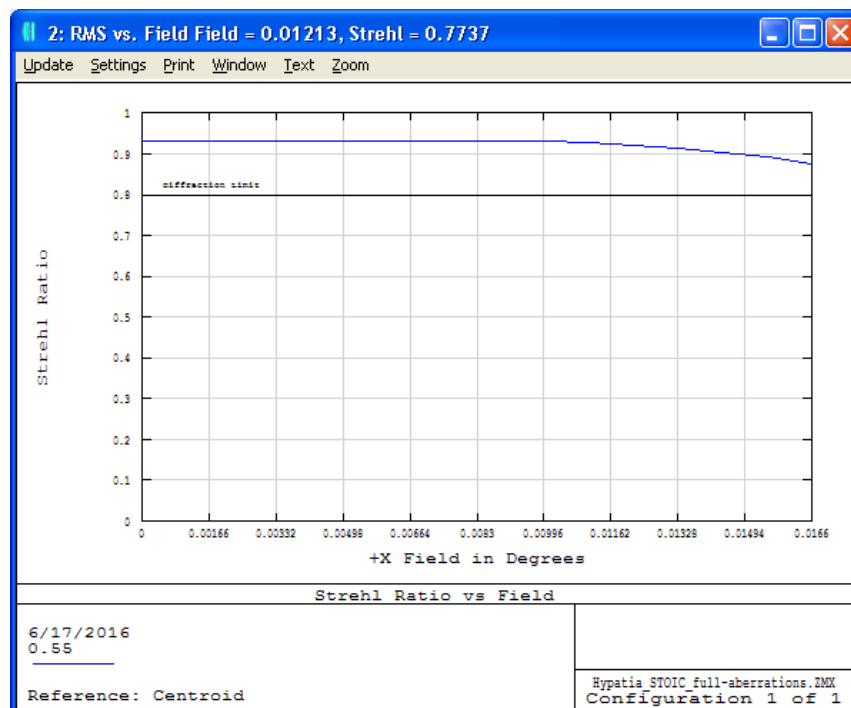
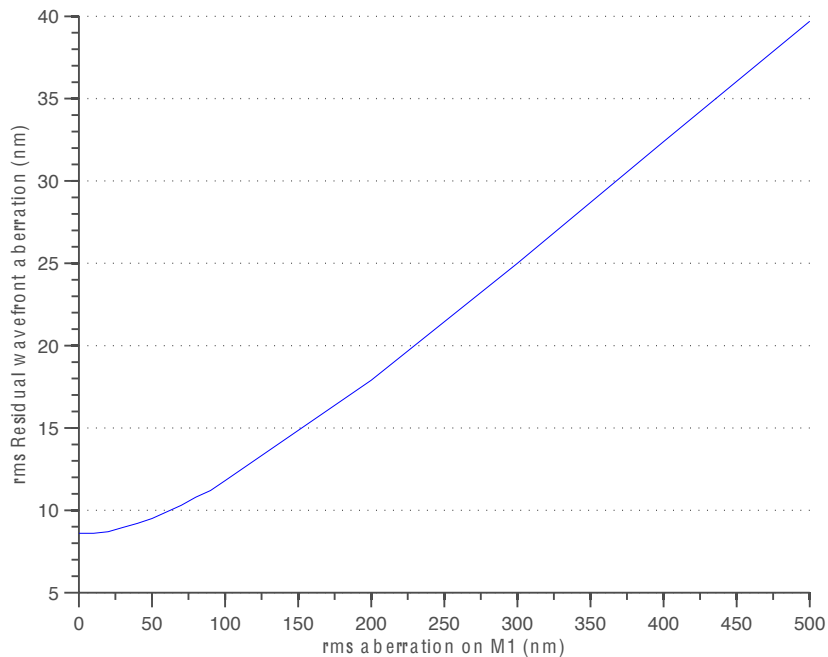


Fig. 2 Strehl ratio at 0.5 microns across field of view following correction of primary mirror aberrations with the deformable mirror.



**Fig. 3 The rms residual wavefront error as a function of rms spherical aberration introduced on M1.**

For larger amplitudes of aberration on the primary mirror, the residual wavefront error increases. For example, Fig. 3 shows the residual as a function of the amplitude of spherical aberration applied to the primary mirror when the correction is spherical aberration on the deformable mirror. For aberrations up to about 100nm (mirror) the residual is similar to wavefront error of the optical configuration. The increasing residual for higher amplitude aberration is mainly due to the imperfect imaging of the primary mirror onto the deformable mirror. The corresponding Strehl ratio is found to be flat over the field of view.

We have also checked the ability of the deformable mirror to correct both misalignment and aberration of the secondary mirror. For example, 100 nm rms Z8 introduced on M2 is corrected by 95 nm Z8 on the deformable mirror with a residual on-axis rms error of 10 nm (about 6 nm over the optical configuration error). The Strehl ratio over the field of view is also well corrected. If the amplitude of the aberration on M2 is increased to 500 nm, the corrected on-axis rms residual error is 20 nm. This would be a very large amplitude of figure error on M2, but it demonstrates that the active optics can be used to relax the figure tolerance for both M1 and M2.

As discussed in the next section, we are in the process of considering alternatives for the wavefront sensing required to control the active optics. The main options we are considering are Shack-Hartmann and phase diversity. The Shack-Hartmann sensor has been tried and tested in many metrology, active and adaptive systems and does not involve moving parts. It may therefore be considered the baseline, low-risk option. Novelities could include the use non-redundant sampling patterns in order to reduce the number of required sub-apertures [2]. Phase diversity allows wavefront aberrations to be estimated from a pair of images with a know phase difference. Typically one image is in focus and the other has about a wave of defocus. Recovery of the wavefront phase requires precise knowledge of the system. If the Fraunhofer approximation may be used to accurately simulate the acquired images, then at least precise knowledge of the pupil shape, including the position and size of the central obscuration, is required. On the other hand, this technique allows for wavefront estimation with a minimum of extra hardware – in the case of the JWST, phase diversity measurements will be obtained with the use of weak lenses in a filter wheel in the near infrared camera, NIRCAM [3]. The fine piston and tip-tilt errors of the JWST segments are estimated, as well as the low-order segment aberrations. Using numerical simulations, Sivaramakrishnam et al. [3] estimate an rms wavefront error of about 10 nm, largely due to detector effects such as cosmetic pixel errors and flat-fielding errors.

### III. ACTIVE OPTICS SIMULATION:

In order to further define the active optics sub-system parameters we have chosen an openware adaptive optics simulation package, 'YAO' (Yorick Adaptive Optics). YAO is a flexible simulation tool developed by Francois Rigaut[5]; it allows the user to simulate many different types of wavefront sensor (Shack-Hartmann, Pyramid, Curvature, Zernike) and deformable mirror (stacked, bimorph, modal, segmented), as well as to set control loop parameters. Multiple sensors and mirrors can be used in order to simulate advanced AO modes such as multi-conjugate adaptive optics. The simulation is written in Yorick, a freely available interpreted programming language, designed for numerical analysis and graphics. It is a Monte-Carlo type simulation; in normal mode of operation, YAO inputs a phase screen simulated to have Kolmogorov statistics (as atmospheric turbulence), applies the telescope pupil and propagates light to the deformable mirror(s) and wavefront sensor(s). The signal from the wavefront sensor is used to determine control signals to be applied to the deformable mirror, and the residual phase used to calculate the corrected point spread function from which can be determined the Strehl ratio, full-width at half-maximum etc.

YAO reads a parameter file in which all of the required system parameters are defined. These include the number of wavefront sensor apertures across the pupil, the image scale of the wavefront sensor, the number of pixels per sub-aperture, the number of actuators and their spacing, parameters defining the shape of the actuator influence function, and loop parameters such as the gain. Operation of YAO involves two steps; (i) initialization of the system and ii) running the control loop. In the initialization, the deformable mirror actuator influence functions are either read from a file or generated, and each actuator is 'poked' in sequence. The resulting wavefront sensor signals are calculated and stored in an array, the Interaction Matrix. In the case of a Shack-Hartmann sensor, the signals are the sub-aperture image displacements in x and y for all the sub-apertures for each actuator poke. Singular value decomposition (SVD) is used to calculate the pseudoinverse of the Interaction Matrix – this gives the Control matrix which is simply multiplied by the wavefront sensor output to give new deformable mirror commands.

We have replaced the atmospheric screens with static combinations of Zernike polynomials and altered the code slightly to read in actuator influence functions produced by Finite Element Analysis. The optical pupil can be defined so that there are actuators outside the pupil as well as inside it. In simulations of the deformable mirror alone, this type of configuration gives the best performance, as it allows precise correction of the aberrations up to the edge of the pupil. However the actuators outside the optical pupil have to be controlled using information from inside the pupil, possibly using extrapolation. We have determined that the control can be precise enough without extrapolation if the mechanical oversizing is not too large i.e. so long as all the actuators have some measurable impact on some sub-apertures. It is necessary to examine how this may limit the brightness of the guide star or the observation time used for sensing. The figure below (Fig. 4) shows the layout in the case where the external pupil diameter is twice the optical pupil diameter (inner circle).

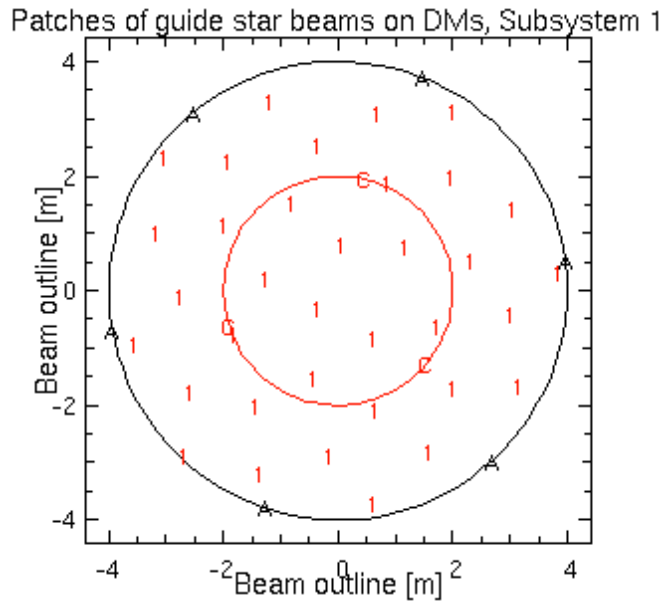


Fig. 4 Map of actuators at Fibonacci positions. The red circle is the optical pupil.

Fig. 5 here shows a sample output from the simulation. The wavefront sensor used in this case is a Shack-Hartmann sensor, with 10 sub-apertures across the pupil, 11 pixels per sub-aperture and a pixel scale of 0.18 arcseconds per pixel. The actuator influence functions were obtained by Finite Element Analysis. The Strehl ratio is constant as the aberration is static. The corrected Strehl ratio is 0.96 at 0.5 microns, corresponding to a residual of 11 nm.

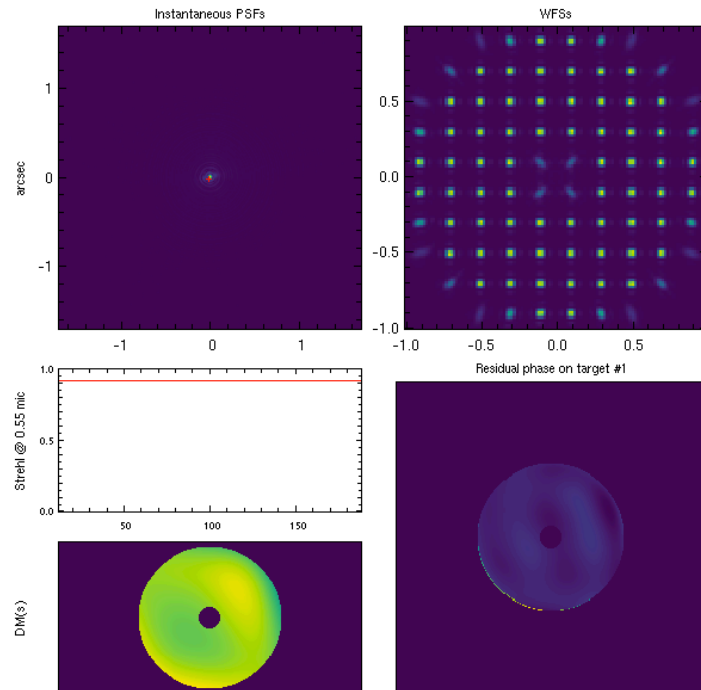
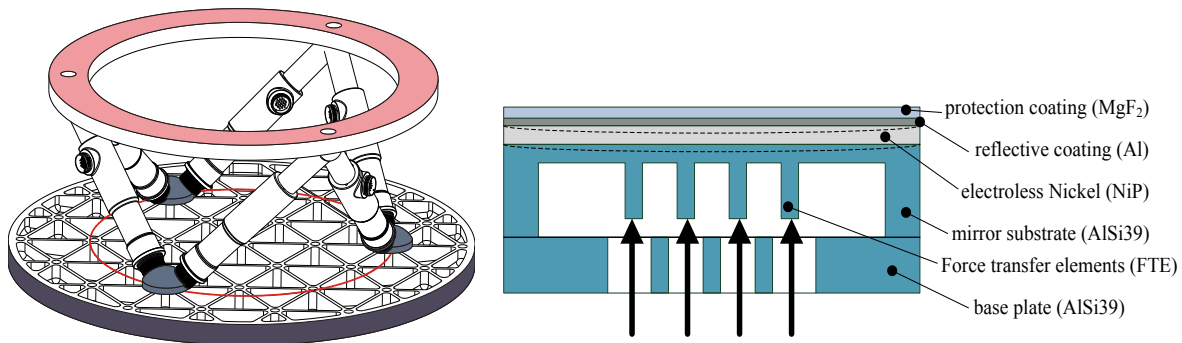


Fig. 5 Graphics output during YAO simulation run. It shows the corrected PSF (top left), Shack-Hartmann image (top right), Strehl ratio evolution, DM shape (bottom left) and the residual wavefront (bottom right).

### III. ACTIVE MIRROR DEVELOPMENT:

The Hypatia telescope will contain two active mirrors - the active secondary and a deformable mirror. The active secondary is intended to compensate for alignment errors such as displacement perpendicular to the optical axis (decentering), tip and tilt as well as defocus. The concept for the substrate of M2 is a convex shaped C/Sic component having a diameter of 600 mm and a weight of 14.3 kg. It is equipped with a light-weighted rib structure, while the circumference is reinforced by a 10 mm thick shell. Six actuators in a hexapod arrangement are used to provide motion with the 6 degree of freedom. Each of them is located at the Bessel diameter (65% of the overall diameter) of the mirror substrate (see the red line in Fig. 6) to ensure low bending while processing and testing under Earth's gravity field. The actuators that are intended to be used for this mirror should provide an accuracy of better than  $1 \mu\text{m}$  to reach the desired lowest tilt error of 1 arcsec and the lowest displacement along the optical axis of about  $1 \mu\text{m}$ . Furthermore, the principle of the actuators should allow maintaining the position without the need for energy, in other words a 'set-and-forget' solution.



**Fig. 6** Left: Drawing of the active secondary mirror with light-weighted mirror substrate and hexapod mounting. Right: Concept of the semi-monolithic deformable mirror.

The deformable mirror which is implemented to compensate for the higher order aberrations is setup as a semi-monolithic component. This means that the mirror body is made of one material but separated into a base plate and the mirror substrate which carries the reflective surface. 36 actuators distributed in a Fibonacci pattern will provide the force which is applied perpendicular to the mirror substrate. Since the force of the actuators is too low to reach sufficient deformation of the mirror substrate, it is amplified using a lever gear. The combination of both, actuators and gears is representatively shown by the black arrows in Fig. 6. Both components of the semi-monolithic body are manufactured with conventional technologies. The material which is an aluminium-silicon-composite is perfectly matched to a nickel plating with regard to the coefficient of thermal expansion. The nickel plating is needed for the single point diamond turning and polishing steps that provide extraordinary high quality surfaces. The residual figure and roughness of the surface must be lower than 20 nm rms or 1 nm rms, respectively. An aluminium coating as well as an MgF<sub>2</sub> coating provide sufficient reflectivity for the desired UVOIR-wave length range and ensure passivation of the mirror surface.

### IV. CONCLUSIONS:

We have presented the concept for a 4m active space telescope. The telescope would be relatively low-risk and low-cost and yet provide excellent image quality down to short wavelengths, with better spatial resolution and light collecting area than the HST. It may be several decades before the launch of projected giant space telescopes, and Hypatia could meanwhile be the flagship space telescope. If combined with a starshade, it could also be used to search for ExoEarths.

We are designing an active optics solution for this telescope. Simulations are being used to determine the parameters of the system, and a laboratory breadboard of the proposed system is being developed. It will provide precise and stable correction of residual telescope aberrations to the level required to take full advantage of diffraction-limited resolution.

REFERENCES

- [1] C. C. Stark, E.J. Cady, M. Clampin, S. Domagal-Goldman, D. Lisman, A.V. Mandell, M.W. McElwain, A. Roberge, T.D. Robinson, D. Savransky, S.B. Shaklan, K.R. Stapelfeldt, "A direct comparison of exoEarth yields for starshades and coronagraphs," *Proc. SPIE*, vol. 9904, 99041U, 2016.
- [2] R. Navarro, J. Arines and R. Rivera, "Wavefront sensing with critical sampling", *Opt. Lett.*, 36, pp 433-435, 2011
- [3] A. Sivaramakrishnan, E.C. Morse, R. Makidon, L.E. Bergeron, S. Casertano, D.F. Figer, D.S.A.D. Atcheson, M.J. Rieke, "Limits on routine wavefront sensing with NIRCcam on JWST", *Proc. SPIE*, vol. 5487, pp908-917, 2004.
- [4] F. Rigaut and M. van Dam., "Simulating Adaptive Optics systems using YAO", Proceedings of the Third AO4ELT conference, eds. S. Esposito and L. Fini, 2013